Macular telangiectasia type 2: quantitative analysis of a novel phenotype and implications for the pathobiology of the disease

Mali Okada, MBBS, MMed*; Catherine A Egan, FRANZCO*†; Tjebo FC Heeren, MD*‡; Adnan Tufail, MD, FRCOphth*; Marcus Fruttiger, PhD‡; Peter M Maloca, MD*§

* Moorfields Eye Hospital NHS Foundation Trust, London, UK

† Department of Ophthalmology, University of Bonn, Bonn, Germany

‡ UCL Institute of Ophthalmology, London, United Kingdom

§ Department of Ophthalmology, University of Basel, Basel, Switzerland

Short Title:

Retinal microcystoid spaces in MacTel 2

Funding:

Supported by the Lowy Medical Research Institute, Sydney, Australia as part of The Macular Telangiectasia Project (MO, CE). AT receives a proportion of funding from the National Institute for Health Research (NIHR) and Biomedical Research Centre at Moorfields Eye Hospital and the University College London Institute of Ophthalmology. The views expressed in the publication are those of the authors and not necessarily those of the Department of Health.

Financial Disclosures:

AT is on the advisory board for Heidelberg engineering (Heidelberg, Germany) and Optovue (Optovue Inc, USA). PM receives fees for lectures from Heidelberg engineering (Heidelberg, Germany)

Address for correspondence:
Peter M Maloca, MD
Moorfields Eye Hospital
162 City Road, London EC1V 2PD
London, United Kingdom
Tel: +44 20 72533411
Fax: +44 20 72534696
peter.maloca@moorfields.nhs.uk

Key words

Macular telangiectasia type 2; spectral domain optical coherence tomography; volume rendering; microcystoid spaces; cystoid macular oedema; microcystic macular oedema; inner nuclear layer cysts; microcysts; microcavitations

Summary Statement

Retinal microcystoid spaces are a novel phenotype of Macular Telangiectasia (MacTel) type 2 on optical coherence tomography. It presents a distinct form of cystoid macular oedema with the pathobiology suggesting possible Müller cell involvement in this disorder.

Abstract

Purpose

To investigate retinal microcystoid spaces in macular telangiectasia (MacTel) type 2 with spectral-domain optical coherence tomography.

Methods

Retrospective review of 135 patients enrolled in the MacTel Natural History Observation and Registry Study at Moorfields Eye Hospital, United Kingdom. 172 eyes from 86 patients who had a comparable scan protocol of at least 30 μm interval were included for analysis. Retinal microcystoid spaces were identified, segmented and metrics analyzed.

Results

From 172 eyes of 86 patients, microcystoid spaces were found in 11 eyes (6.4%) from 8 patients (9.3%). The mean number of microcystoid spaces per eye was 12.9 ± 18.2. The majority were located in the inner nuclear layer. The inferonasal quadrant of the macula was the least commonly affected region. Microcystoid spaces were distributed entirely within the assumed MacTel area on blue light reflectance imaging in all but two eyes (4 of 142 microcysts). Median diameter of the microcystoid spaces was 31 μm (range 15 to 80 μm).

Conclusion

Microcystoid spaces as a phenotype of MacTel should be considered in the differentials for microcystic oedema. Understanding the pathogenesis of these lesions may provide further insight into the role of Müller cell dysfunction in this disorder.

Introduction

Macular telangiectasia type 2 (MacTel) is a rare degenerative disorder of the central retina. The disease causes progressive central vision loss and is typically diagnosed in patients between the age of fifty to sixty, who describe problems with reading vision often for years prior to measurable visual acuity changes.[1–3]

The exact cause of the disease remains unclear. Although the early description of the disease by Gass and Oyakawa suggested an underlying vascular aetiology,[4] it is now thought to be more consistent with a neurodegenerative process. Recent histopathological studies have demonstrated a striking depletion of Müller cells in the central retina in the same distribution as macular pigment reduction, pointing towards neuroglial loss as critical in this disorder, leading to structural and functional impairment in cone and rod photoreceptors.[5–8]

In recent years, optical coherence tomography imaging (OCT) has become an increasingly valuable diagnostic tool, providing further phenotyping of the disease. Characteristic findings include hyporeflective spaces of the inner and outer neurosensory retina, ellipsoid zone (EZ) disruption, hyperreflective lesions from pigment migration, as well as foveal atrophy in late stage disease.[9–13] Typically the central macular retinal thickness remains normal or may be reduced despite presence of angiographic leakage.[14]

In addition to these imaging findings, optical coherence tomography angiography (OCTA) has also recently identified the presence of small retinal hyporeflective spaces in MacTel patients. Termed ‘microcavitations’, these spaces were defined as

an optically empty space less than 250 μm in dimension and were frequently distributed around right-angle venules but were also present in areas without obvious vascular changes on OCTA.[15] The microcavitations were mainly located in the inner retina, predominantly in the ganglion cell layer (GCL), inner nuclear layer (INL) as well as Henle's fibre layer. Similar microcavitations, described with varying terminology by others, have also been identified in a case report using light microscopy [16], as well as on adaptive optics scanning laser ophthalmoscopy (AOSLO) (meeting abstract).[17]

Aside from MacTel, microcystoid changes of the macula have been described in a variety of hereditary or acquired optic neuropathies and predominantly occur in the INL on OCT.[18–21] These lesions are not observed in normal eyes and might correspond to the microcystoid spaces seen in MacTel. The presence of microcystoid spaces in patients with MacTel type 2 may further provide clues to the pathogenesis of the disorder. In this study, we present a quantitative analysis of the metrics and distribution of microcystoid spaces with spectral-domain OCT (SD-OCT).

Methods

Study Design

This was a retrospective review of the OCT images of 135 patients diagnosed with MacTel type 2 at Moorfields Eye Hospital, London UK and who were enrolled in the MacTel Natural History Observation and Registry study. All patients had fundoscopy, SD-OCT, blue light reflectance (BLR) imaging, dual wavelength autofluorescence for macular pigment optical density (MPOD) mapping and fluorescein angiography as part of the study protocol.[22] Only patients who had SD-OCT volume scans with a minimum of 30 μm interslice distance were included for analysis. Exclusion criteria were any clinical or electrodiagnostic evidence of concomitant optic nerve disease, diabetic retinopathy, and poor imaging quality. Retrospective OCT data from eight eyes of four healthy controls were also included for comparative purposes. Two graders (PM and MO), masked to patient identifying details and disease status, graded all scans meeting eligibility criteria for the presence of visible retinal microcystoid spaces. Macular microcystoid spaces were defined in this study as small hyporeflective spaces that were non-contiguous with typical larger inner or outer retinal cavitations. The terminology 'microcystoid space' is preferred here as it applies to cystoid-like changes seen on imaging. The study was approved by the local institutional review board and conducted according to the tenets of the Declaration of Helsinki. Informed consent was obtained from all study participants.

OCT and BLR Imaging and Image Analysis

OCT imaging was acquired using Heidelberg Spectralis® HRA2 system (Heidelberg Engineering, Heidelberg, Germany). The scan pattern for patients was between 3.8 x 2.5 x 1.9 mm to 4.4 x 2.9 x 1.9 mm. B-scans ranged from 49 to 261 scans per volume,

with imaging averaging for 8 – 12 scans and an interslice distance of 11-30 μm. The scan pattern for all healthy controls was raster lines 4.5 × 3.0 × 1.9 mm, 261 B-Scans, interslice distance of 11 μm, averaging 20 scans using the automatic averaging and tracking feature.

In patients where microcystoid spaces were visually identified, segmentation of all hyporeflective cystoid spaces present in that scan was performed using image-processing software AMIRA 6.1 (Materials & Structural Analysis, Merignac, France). Microcystoid spaces were segmented through thresholding of pixel intensity. A threshold from 0 to 50 grey-scale units (scale 0 to 255) showed reasonably well-separated lesions, further identifying smaller microcystoid spaces that were not visible initially on manual identification. Image artifact from vessel shadowing was excluded. Microcystoid volumes were also measured. Based on a presumed sphere model, data for diameter and surface area were calculated. Average central foveal thickness was recorded using the central area on the Early Treatment Diabetic Retinopathy Study grid area on Heidelberg Eye Explorer viewing module software.

In patients with microcystoid lesions, the location of each lesion in relation to individual retinal layers was recorded on the B-scans according to the International Nomenclature for OCT consensus.[23] The spatial distribution of the microcystoid spaces was also compared to the theoretical MacTel area as seen on BLR imaging, which has been shown to correspond to the area of macular pigment loss as measured by dual wavelength autofluorescence[24] and on histology.[6] For this purpose, open source imaging software ImageJ (v1.467 (ref - Rasband, W.S., ImageJ, U. S. National Institutes of Health, Bethesda, Maryland, USA, https://imagej.nih.gov/ij/, 1997-2016) was used to overlay the patient's scanning laser ophthalmoscopy image (SLO) using

the metric of the SLO image and transferred onto the aligned BLR image with Adobe Photoshop CC 2017 (Adobe Systems, San José, United States). Finally, identified microcystoid spaces were exported and overlaid on the patient's BLR images with AMIRA software to analyse the distribution with respect to the MacTel area and the distribution in quadrants centred on the fovea.

Results

One hundred and thirty-five patients were enrolled at Moorfields Eye Hospital in the MacTel Natural History Observation and Registry study. Of these, 86 (64%) patients or 172 eyes had at least one volume scan meeting the 30 μm minimum interslice inclusion criteria. In total, 11 eyes (6.4% of eligible eyes) from 8 patients were identified as having microcystoid spaces as assessed by two masked graders. The demographic and clinical details of the patients are described in Table 1. Mean age of the patients was 53.1 years (range 37 – 71 years) and mean visual acuity was 0.16 LogMAR units (range 0.0 – 0.78 LogMAR units; equivalent to 20/28 Snellen acuity). Average central foveal thickness using the ETDRS grid was normal in all eyes (mean 249 ± 22 μm). None of the patients had pigment plaques or evidence of subretinal neovascularisation. One of the patients had highly asymmetric disease with typical BLR and macular pigment changes in the affected eye but no clinical or imaging features of MacTel in the fellow eye.

When present, the mean number of microcystoid spaces per eye was 12.9 ± 18.2 (range 1 to 61 microcystoid spaces) with a total 142 microcystoid spaces across all 11 eyes. None of the control eyes (n = 8) had microcystoid spaces on OCT imaging

either by manual grading with two masked graders or with image processing segmentation using the same threshold criteria. Median volume of the microcystoid spaces was 15,146 μm^3 (range 1,829 to 27,0724 μm^3) (Figure 1), median surface area was 2,960 μm^3 (range 723 to 20,238 μm^2) and median diameter was 31 μm (range 15 to 80 μm). Eighty-three percent of the assessed lesions had a volume between 16,000 and 44,000 μm^3.

Location of the Microcystoid Spaces within Retinal Layers

Each microcystoid space was assessed according to the predominant retinal layer or zone it was located within on B-scan segmentation. The majority were located within the INL (42%, n = 59) followed by the outer plexiform layer (OPL) and GCL (Figure 2 and 3). No microcystoid spaces were found posterior to the external limiting membrane.

Distribution of Microcystoid Spaces

Microcystoid spaces were seen in all quadrants of the macula however the infero-nasal quadrant was the least common quadrant (inferonasal: 15% versus superonasal: 35%). There was no difference across the vertical meridian with an equal number of microcystoid spaces in the temporal (50%, n = 71) as compared to the nasal half of the macula. There was no direct correlation between the location of microcystoid spaces and the areas of early hyperfluorescence on fundus fluorescein angiogram.

The microcystoid spaces were distributed within the parafoveal region of the macula (Figures 3 and 4). The spatial location of the microcystoid spaces was analysed and compared to the assumed MacTel area for each patient as defined by the area of

increased reflectance on BLR imaging. In 9 of 11 eyes (82 %) the microcystoid spaces were all entirely contained within the MacTel area. In one eye, the peripheral microcystoid spaces (2 of 61 lesions in that eye) were located temporally, slightly outside the MacTel area (Figure 4). In the second eye, the peripheral lesions (2 of 7 microcystoid spaces in that eye) were in the inferonasal area of the perifoveal region where there was no increased BLR.

Discussion

This paper confirms and extends previously published reports[15,16] of the presence of macular microcystoid spaces in a separate patient cohort with MacTel type 2 and the findings are using a different imaging modality (SD-OCT rather than OCTA). Furthermore, this study provides a novel quantitative analysis and a detailed examination of the distribution of the microcystoid spaces with respect to the so-called MacTel area, defined here as the area of increased parafoveal BLR. We demonstrate that the microcystoid spaces were concentrated in the INL and OPL, occurring in an oval parafoveal region that largely correlated with the MacTel area. Interestingly, a small number of the lesions extended slightly beyond this hypothetical MacTel area boundary. This might point towards MacTel as a more extensive macular disease than previously thought. It may also suggest that these microcystoid spaces can show up earlier than macular pigment changes as seen in the patient with microcystoid spaces in the inferonasal area where there was sparing on BLR and macular pigment optical density mapping. However, it is also possible that these more peripheral microcystoid spaces are different from the ones within the MacTel area and may even be present in normal aged eyes. We did not see them however in our normal

healthy controls or in the fellow unaffected eye of the patient with asymmetric disease.

Microcystic cavities in MacTel type 2 were first described in a histopathological case report in 1980, when the disease was still described as 'parafoveal retinal telangiectasis'.[16] Using light and electron microscopy, the authors examined an eye with features of MacTel type 2 which had undergone exenteration, and found 'microcystic changes' in the temporal macula. Microcystic cavities were predominantly noted in the INL and OPL, and were associated with thickening of the temporal macula up to 3mm distance from the fovea. Although histology and OCT are difficult to compare, the retinal layer location and distribution of these 'microcystic cavities' are similar to the microcystoid spaces described on retinal imaging in our study and also reported by Spaide and colleagues.[15]

On microscopy the microcystic cavities reported by Green et al. were not empty spaces but rather contained lightly-staining fibrillar material.[16] Microcystic cavities however were not evident in more recent histological studies.[5,6] This may be due to differences in disease stage of the patients, which were more advanced in these latter reports. Larger cystoid cavities have been identified but were structurally empty on haematoxylin-eosin staining.

It is also possible that the microcystoid spaces seen here on OCT correspond to the inner retinal 'spherical microcysts' in MacTel type 2 on AOSLO (ARVO abstract).[17] The microcysts described ranged from 30 to 100 μm in size and were all located within the inner retina, although detail of specific retinal layer involvement was not

provided. Interestingly, the authors found spherical microcysts in 7 of 14 patients, also with early stage disease. Assuming these are similar entities, they found a much higher prevalence. This may be due to differences in the resolution of the imaging method, with our cohort including patients with minimum 30 μm interval scans, and smaller microcystoid spaces may have been missed. This is also possible given the median diameter of microcystoid spaces in this present study was 31μm size only. Interestingly, the patient with 11 μm interval scans did not have a higher rate of microcystoid spaces so other factors may be relevant in addition to resolution scan interval.

The microcystoid spaces in MacTel may also be similar in mechanism to the 'macular microcysts' involving the INL in a variety of optic neuropathies.[18,21,25,26] The mechanism for this is still unclear, as conventional teaching would suggest that optic neuropathy should result in GCL thinning alone due to axonal injury. One proposed theory to explain the INL involvement in optic neuropathy entails retrograde synaptic degeneration of optic nerve axons with secondary degeneration of Müller neuroglial cells.[18,20,26] Vitreomacular adhesion with or without traction may also contribute to inward exerting forces on the INL.[26–28] Given the key finding of central Müller cell depletion in MacTel on histopathology,[5,6] it is possible that Müller cell dysfunction may also be responsible for the microcystoid disease phenotype presented here. Müller cells span the entire neuroretina and are important not only as a scaffold but also in the osmotic regulation of the retina.[29] Further evidence of this is suggested by the presence of INL microcystic changes in 20% of patients with neuromyelitis optica (NMO) who had a history of previous optic neuritis.[21] Interestingly, retinal Müller

cells are rich in aquaporin-4 water channels, with antibodies against these channels implicated in the immunopathogenesis of NMO-spectrum disorder.

Microcystoid spaces in this present study were distributed in the parafoveal region with the inferior-nasal quadrant of the macular being the least common quadrant to be affected. Although most eyes showed increased reflectance infero-nasally on BLR imaging, there is a predilection for sparing of that area in MacTel.[30] Analysis of the location of the microcystoid spaces in relation to the theoretical MacTel area revealed most were contained within the area of parafoveal increased reflectance or within the surrounding band of decreased reflectance (corresponding to the outer halo of macular pigment accumulation on MPOD mapping). However in 2 eyes, a few microcystoid spaces extended more peripherally. This is the first demonstration of pathology in MacTel that appears beyond this confined oval area, which is thought to have a boundary of approximately ≤ 5 – 7° horizontally and ≤ 5° vertically on imaging and histologic analysis.[6,24,31,32] This is in contrast to the findings of Spaide et al. where microcavitations were all reportedly located within the MacTel area.[15] This difference may be due to the imaging modality used to estimate the MacTel area (MPOD versus BLR) or the use of different scan protocols (OCTA versus OCT).

There are several limitations to this study. This was a retrospective study and although we only included images with less than 30 μm interslice distance, scanning protocols varied between patients. It is possible that smaller microcystoid spaces may have been missed and this could explain the difference in frequency of lesions found in this series compared to the Spaide et al cohort.[15] The findings here are also at a single time point in the disease and microcystoid spaces may not necessarily be seen

at every scan date. Further confirmation of these findings in a larger cohort and analysis of variability with time would be interesting. It is also unclear at this stage why this microcystoid phenotype is seen more commonly in early disease and whether it represents a distinct phenotype. Examination of the relationship between microcystoid spaces and retinal function would be valuable. There are also very few normative datasets available to examine whether microcystoid spaces may be present in normal eyes. We attempted to address this by performing the same thresholding and segmentation in our control eyes. The control group had an even more robust scanning protocol with interslice distance of only 11 μm and no microcystoid spaces were seen in any normal eyes or in the fellow eye of the patient with asymmetric disease.

In summary, we present quantification and analysis of microcystoid spaces in MacTel type 2 using SD-OCT imaging. Awareness of microcystoid spaces as part of the disease phenotype of MacTel type 2 is important when assessing differentials for microcystoid changes in macular diseases. In this study, microcystoid spaces were present often in early stage disease and were not associated with any retinal thickening as would be expected in traditional vascular causes of microcystic oedema.

We also demonstrate that although the majority of microcystoid spaces are contained within the MacTel area, small numbers can extend slightly beyond this region. Our findings add weight to the evidence suggesting Müller cell involvement in the pathogenesis of this disease. If confirmed, presence and volume of microcystoid spaces may also be a useful biomarker of disease activity. The use of a quantitative imaging method may have value as an endpoint in treatment trials or have prognostic

implications for MacTel and other disorders associated with presumed Muller cell degeneration.

References

1. Heeren TFC, Holz FG, Charbel Issa P. First symptoms and their age of onset in macular telangiectasia type 2. *Retina* 2014;34(5):916-919.

2. Lamoureux EL, Maxwell RM, Marella M, Dirani M, Fenwick E, Guymer RH. The longitudinal impact of macular telangiectasia (MacTel) type 2 on vision-related quality of life. *Invest Ophthalmol Vis Sci* 2011;52(5):2520-2524.

3. Clemons TE, Gillies MC, Chew EY, et al. The National Eye Institute Visual Function Questionnaire in the Macular Telangiectasia (MacTel) Project. *Invest Ophthalmol Vis Sci* 2008;49(10):4340-4346.

4. Gass JD, Oyakawa RT. Idiopathic juxtafoveolar retinal telangiectasis. *Arch Ophthalmol* 1982;100(5):769-780.

5. Powner MB, Gillies MC, Tretiach M, et al. Perifoveal muller cell depletion in a case of macular telangiectasia type 2. *Ophthalmology* 2010;117(12):2407-2416..

6. Powner MB, Gillies MC, Zhu M, Vevis K, Hunyor AP, Fruttiger M. Loss of Muller's cells and photoreceptors in macular telangiectasia type 2. *Ophthalmology* 2013;120(11):2344-2352.

7. Schmitz-Valckenberg S, Fan K, Nugent A, et al. Correlation of functional impairment and morphological alterations in patients with group 2A idiopathic juxtafoveal retinal telangiectasia. *Arch Ophthalmol* 2008;126(3):330-335.

8. Wang Q, Tuten WS, Lujan BJ, et al. Adaptive optics microperimetry and OCT images show preserved function and recovery of cone visibility in macular telangiectasia type 2 retinal lesions. *Invest Ophthalmol Vis Sci*. 2015;56(2):778-786.

9. Charbel Issa P, Gillies MC, Chew EY, et al. Macular telangiectasia type 2. *Prog Retin Eye Res* 2013;34:49-77.

10. Gaudric A, Ducos de Lahitte G, Cohen SY, Massin P, Haouchine B. Optical coherence tomography in group 2A idiopathic juxtafoveolar retinal telangiectasis. *Arch Ophthalmol* 2006;124(10):1410-1419.

11. Gupta V, Gupta A, Dogra MR, Agarwal A. Optical coherence tomography in group 2A idiopathic juxtafoveolar telangiectasis. *Ophthalmic Surg Lasers Imaging* 2005;36(6):482-486.

12. Barthelmes D, Gillies MC, Sutter FKP. Quantitative OCT analysis of idiopathic perifoveal telangiectasia. *Invest Ophthalmol Vis Sci* 2008;49(5):2156-2162.

13. Sallo FB, Peto T, Egan C, et al. The IS/OS junction layer in the natural history of type 2 idiopathic macular telangiectasia. *Invest Ophthalmol Vis Sci* 2012;53(12):7889-7895.

14. Paunescu LA, Ko TH, Duker JS, et al. Idiopathic Juxtafoveal Retinal Telangiectasis: New Findings by Ultrahigh-Resolution Optical Coherence Tomography. *Ophthalmology* 2006;113(1):48-57.

15. Spaide RF, Suzuki M, Yannuzzi LA, Matet A, Behar-Cohen F. Volume-Rendered Angiographic and Structural Optical Coherence Tomography Angiography of Macular Telangiectasia Type 2. *Retina* 2017;37(3):424-435

16. Green WR, Quigley HA, De la Cruz Z, Cohen B. Parafoveal retinal telangiectasis. Light and electron microscopy studies. *Trans Ophthalmol Soc U K* 1980;100(Pt 1):162-170.

17. Roorda A, Lujan B, Ratnam K, et al. Microscopic Retinal Structure in Macular Telangiectasia. *Invest Ophthalmol Vis Sci* 2013;54(15):3606-3606.

18. Abegg M, Zinkernagel M, Wolf S. Microcystic macular degeneration from optic neuropathy. *Brain J Neurol* 2012;135(Pt 12):e225.

19. Abegg M, Dysli M, Wolf S, Kowal J, Dufour P, Zinkernagel M. Microcystic macular edema: retrograde maculopathy caused by optic neuropathy. *Ophthalmology* 2014;121(1):142-149

20. Wolff B, Basdekidou C, Vasseur V, Mauget-Faysse M, Sahel J-A, Vignal C. Retinal inner nuclear layer microcystic changes in optic nerve atrophy: a novel spectral-domain OCT finding. *Retina*. 2013;33(10):2133-2138.

21. Gelfand JM, Cree BA, Nolan R, Arnow S, Green AJ. Microcystic inner nuclear layer abnormalities and neuromyelitis optica. *JAMA Neurol* 2013;70(5):629-633.

22. Clemons TE, Gillies MC, Chew EY, et al. Baseline characteristics of participants in the natural history study of macular telangiectasia (MacTel) MacTel Project Report No. 2. *Ophthalmic Epidemiol* 2010;17(1):66-73.

23. Staurenghi G, Sadda S, Chakravarthy U, Spaide RF. Proposed lexicon for anatomic landmarks in normal posterior segment spectral-domain optical coherence tomography: the IN*OCT consensus. *Ophthalmology* 2014;121(8):1572-1578.

24. Charbel Issa P, Berendschot TTJM, Staurenghi G, Holz FG, Scholl HPN. Confocal blue reflectance imaging in type 2 idiopathic macular telangiectasia. *Invest Ophthalmol Vis Sci* 2008;49(3):1172-1177.

25. Saidha S, Sotirchos ES, Ibrahim MA, et al. Microcystic macular oedema, thickness of the inner nuclear layer of the retina, and disease characteristics in multiple sclerosis: a retrospective study. *Lancet Neurol* 2012;11(11):963-972.

26. Lujan BJ, Horton JC. Microcysts in the inner nuclear layer from optic atrophy are caused by retrograde trans-synaptic degeneration combined with vitreous traction on the retinal surface. *Brain J Neurol* 2013;136(Pt 11):e260.

27. Sigler EJ. Microcysts in the inner nuclear layer, a nonspecific SD-OCT sign of cystoid macular edema. *Invest Ophthalmol Vis Sci* 2014;55(5):3282-3284.

28. Barboni P, Carelli V, Savini G, Carbonelli M, La Morgia C, Sadun AA. Microcystic macular degeneration from optic neuropathy: not inflammatory, not trans-synaptic degeneration. *Brain J Neurol* 2013;136(Pt 7):e239

29. Reichenbach A, Bringmann A. New functions of Muller cells. *Glia* 2013;61(5):651-678.

30. Zeimer MB, Kromer I, Spital G, Lommatzsch A, Pauleikhoff D. Macular telangiectasia: patterns of distribution of macular pigment and response to supplementation. *Retina* 2010;30(8):1282-1293.

31. Helb H-M, Charbel Issa P, VAN DER Veen RLP, Berendschot TTJM, Scholl HPN, Holz FG. Abnormal macular pigment distribution in type 2 idiopathic macular telangiectasia. *Retina* 2008;28(6):808-816.

32. Zeimer MB, Padge B, Heimes B, Pauleikhoff D. Idiopathic macular telangiectasia type 2: distribution of macular pigment and functional investigations. *Retina* 2010;30(4):586-595.

Figures

Figure 1.

Volume of the microcystoid spaces in MacTel type 2. Eighty-three percent of the assessed lesions had a volume between 16,000 and 44,000 μm^3.

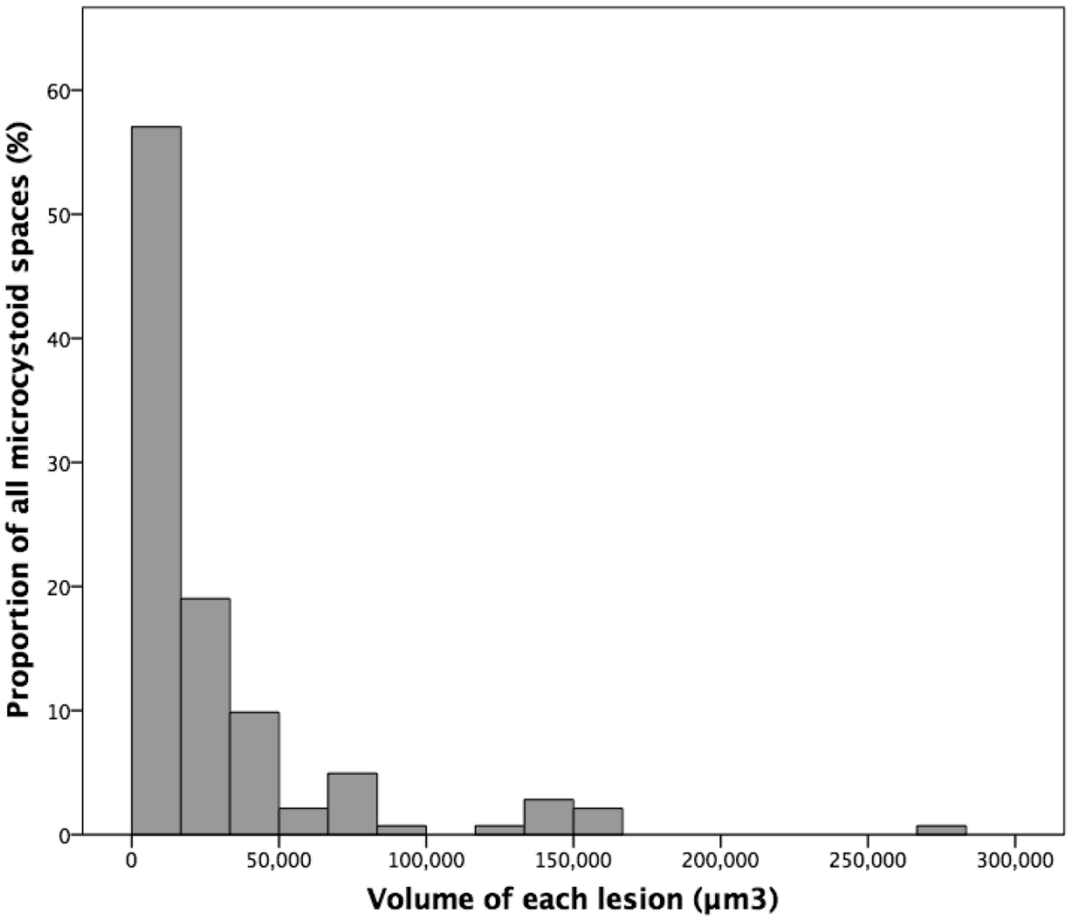

Figure 2.
Location of microcystoid spaces within the retinal layers, showing a predilection for the INL, OPL and GCL. NFL: nerve fibre layer; GCL: ganglion cell layer; IPL: inner plexiform layer; INL: inner nuclear layer; OPL: outer plexiform layer; ONL: outer nuclear layer; HFL: Henle's fibre layer; ELM: external limiting membrane; MZ: myoid zone; EZ: ellipsoid zone; IZ: interdigitation zone; RPE: retinal pigment epithelium

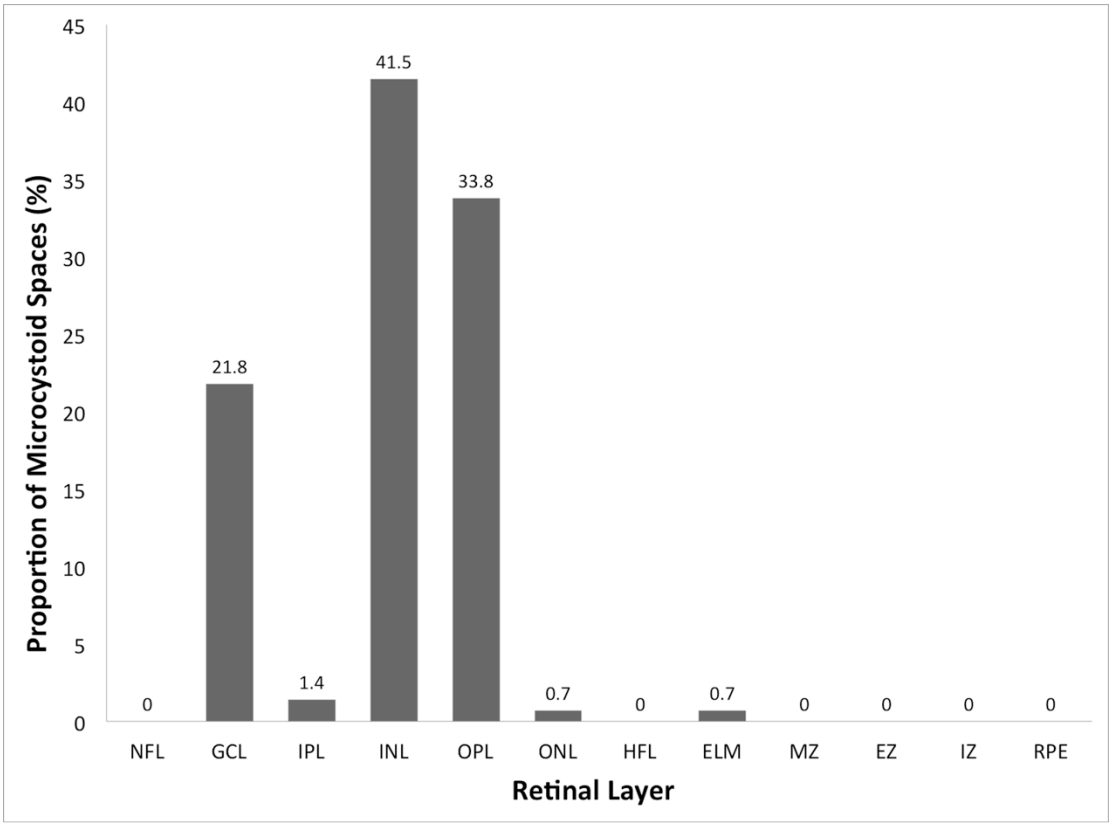

Figure 3. Macular microcystoid spaces on spectral-domain optical coherence tomography imaging in two patients with MacTel 2. Left: overlay of microcystoid spaces (white dots) on the patient's blue light reflectance imaging. Right: Corresponding B-scan with microcystoid spaces in inner nuclear layer (arrows) and ganglion cell layer (arrow head).

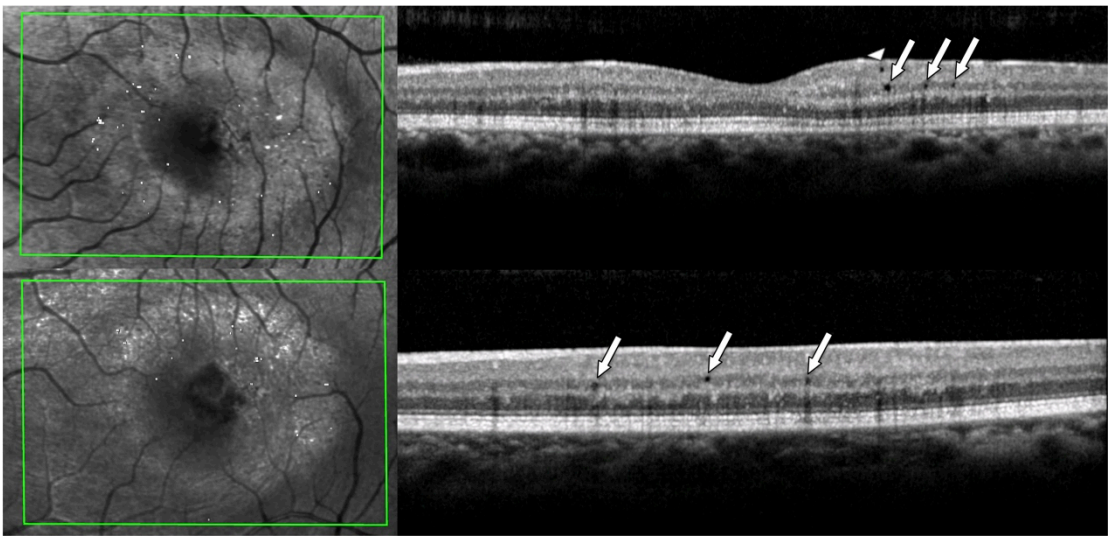

Figure 4. Multimodal imaging of the right eye of a 37 year old man with MacTel type 2 (Patient 1 in Table). (A) Macula pigment optical density map showing characterstic central depletion as a darker area surrounded by a brighter ring of persisting macular pigment. (B) Late phase fluorescein angiography demonstrating parafoveal hyperfluorescence. (C) Spectral-domain optical coherence tomography scan through fovea with visible microcystoid spaces (arrow) in inner nuclear layer and outer plexiform layer. (D) Overlay of all segmented microcystoid spaces (white dots) against the area of increased parafoveal reflectance on blue light reflectance image. Note the two temporal microcytoid spaces that are present beyond the area of increased reflectance (arrows).

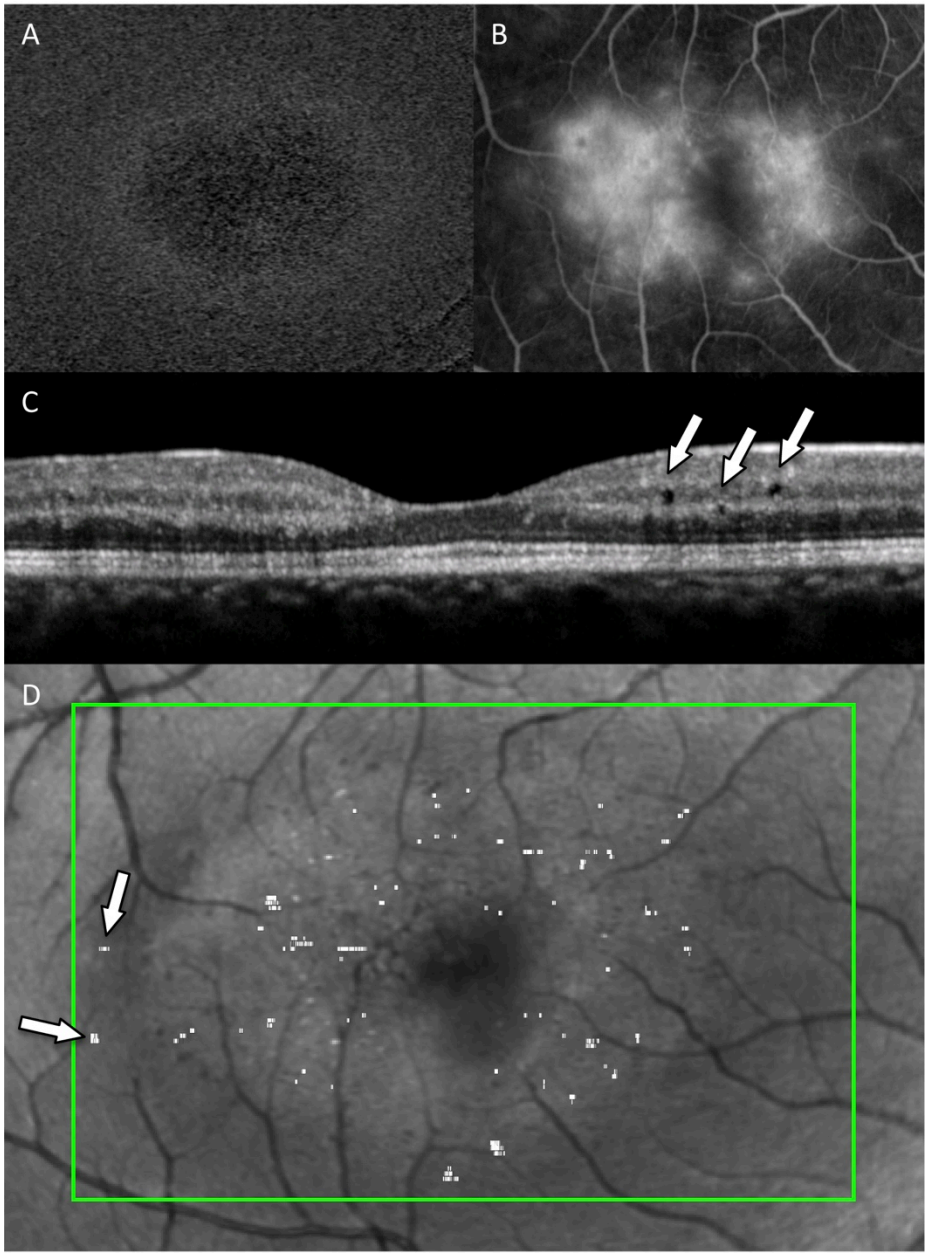

Table. Summary of the clinical and demographic features of identified patients.

ID	Age	Gender	Eye	Diabetic Retinopathy	Number of Microcystoid Spaces	CFT (μm)	Other OCT lesions
1	37	M	Right	No	61	270	Irregular reflectivity but no break of EZ
			Left	No	30	256	Irregular reflectivity but no break of EZ
2	45	F	Right	No	7	244	Small parafoveal flat inner retinal HC
			Left	No	2	234	Irregular reflectivity of ONL
3	52	M	Right	No	8	258	Irregular reflectivity but no break of EZ
4	66	F	Right	No	1	241	Small EZ break temporally
			Left	No	2	241	Small parafoveol flat inner retinal HC temporally
5	49	M	Right	No	1	292	Large inner retinal HC
6	53	F	Left	No	17	240	Large inner retinal HC; EZ disruption
7	52	F	Right	No	2	204	Large inner retinal HC; Irregular EZ but no break
8	71	M	Left	No	11	264	Small flat inner retinal HC in the foveola, small EZ break temporally

ID: Patient identification number; CFT: Average central foveal thickness on ETDRS grid with Heidelberg Explorer; OCT: Optical coherence tomography; HC: Hyporeflective cavities; EZ: ellipsoid zone; ONL: outer nuclear layer.